8. Xu W, Bergsbaken T, Edelblum KL. The multifunctional nature of CD103 (αEβ7 integrin) signaling in tissue-resident lymphocytes. *Am J Physiol Cell Physiol* 2022;323:C1161–C1167.
9. Djenidi F, Adam J, Goubar A, Durgeau A, Meurice G, de Montpréville V, *et al.* $CD8^+CD103^+$ tumor-infiltrating lymphocytes are tumor-specific tissue-resident memory T cells and a prognostic factor for survival in lung cancer patients. *J Immunol* 2015;194:3475–3486.
10. Selman M, Pardo A, Barrera L, Estrada A, Watson SR, Wilson K, *et al.* Gene expression profiles distinguish idiopathic pulmonary fibrosis from hypersensitivity pneumonitis. *Am J Respir Crit Care Med* 2006;173: 188–198.
11. Richmond JM, Strassner JP, Zapata L Jr, Garg M, Riding RL, Refat MA, *et al.* Antibody blockade of IL-15 signaling has the potential to durably reverse vitiligo. *Sci Transl Med* 2018;10:eaam7710.

Copyright © 2023 by the American Thoracic Society

Check for updates

## *De Novo* Generation of Pulmonary Ionocytes from Normal and Cystic Fibrosis Human Induced Pluripotent Stem Cells

Ruobing Wang[1,2,3], Chantelle Simone-Roach[1,2,3], Jonathan Lindstrom-Vautrin[2], Feiya Wang[2], Stuart Rollins[1,3], Pushpinder Singh Bawa[2], Junjie Lu[4], Yang Tang[3], Mary Lou Beermann[2,5], Thorsten Schlaeger[3], John Mahoney[4], Steven M. Rowe[6], Finn J. Hawkins[2,5], and Darrell N. Kotton[2,5,7]

[1]Division of Pulmonary Medicine, Boston Children's Hospital, Boston, Massachusetts; [2]Center for Regenerative Medicine of Boston University and Boston Medical Center, Boston, Massachusetts; [3]Department of Medicine, Harvard Medical School, Boston, Massachusetts; [4]Cystic Fibrosis Foundation Therapeutics Laboratories, Lexington, Massachusetts; [5]The Pulmonary Center and Department of Medicine and [7]Department of Pathology & Laboratory Medicine, Boston Medical Center, Boston University School of Medicine, Boston, Massachusetts; and [6]Department of Medicine and the Gregory Fleming James Cystic Fibrosis Research Center, University of Alabama at Birmingham, Birmingham, Alabama

ORCID IDs: 0000-0003-0277-8329 (R.W.); 0000-0001-9045-0133 (S.M.R.); 0000-0002-9604-8476 (D.N.K.).

*To the Editor*:

The advent of single-cell RNA sequencing (scRNA-Seq) has resulted in new lung cell atlases and the recognition of previously undescribed lung cell types (1–3). Particularly relevant for epithelial biologists are recent reports of a rare population of CFTR (cystic fibrosis transmembrane conductance regulator)-rich airway epithelial cells, marked by the expression of transcription factors *FOXI1* (forkhead box I1) and *ASCL3* (achaete-scute homolog 3) (1, 2). Given their similarity to ionocytes previously described in other organisms or tissues, such as in *Xenopus* larva skin (4, 5), these cells were termed "pulmonary ionocytes." Pulmonary ionocytes are present in both mouse and human airways, representing ∼1% of all airway epithelial cells. Although a growing literature shows that ionocytes express the highest levels of *CFTR* mRNA in the respiratory tree, their functional relevance remains controversial (6), and new human model systems are needed to examine their developmental origins and biological roles. Here we report the *de novo* derivation of pulmonary ionocytes through the developmental directed differentiation of human induced pluripotent stem cells (iPSCs). We recently published methods for the differentiation of iPSCs into cells expressing a molecular and functional phenotype reminiscent of airway basal cells (7). As with their *in vivo* correlates, iPSC-derived airway basal-like cells (iBCs) exhibit functional features of tissue-resident airway stem cells, given their ability to indefinitely self-renew or undergo multipotent differentiation into airway secretory or multiciliated cells, both *in vitro* and *in vivo*, in tracheal xenograft models (7). In our original publication, we did not detect the presence of cells resembling ionocytes (7). Given prior studies demonstrating that primary basal cells *in vivo* can serve as precursors for pulmonary ionocytes (2), we have reexamined the differentiation repertoire of iBCs after a modification of our differentiation protocol (Figure 1A). We report here that after additional expansion of iBCs including two rounds of sequential sorting on the cell surface protein, NGFR (nerve growth factor receptor), iBCs can give rise to ionocytes in addition to our previously reported trilineage airway epithelial differentiation repertoire. For example, after two rounds of NGFR sorting, iBCs maintained in three-dimensional cultures in our previously published basal cell medium (7) can be transferred to two-dimensional air–liquid interface (ALI) culture (in our previously published ALI protocol [7]), giving rise after 3 weeks to basal, secretory, multiciliated, and ionocyte progeny (Figure 1B).

Using this modified protocol, we performed duplicate differentiations of four iPSC clones into ALI cultures ($n = 8$ total differentiations of two iPSC clones from two distinct cystic fibrosis donors carrying homozygous F508del CFTR mutations and two clones consisting of their progeny after mutation correction by CRISPR gene editing). We profiled the resulting cells by scRNA-Seq, generating eight datasets representing the global transcriptomes of 19,255 cells (Gene Expression Omnibus accession numbers GSE203006, GSE203007, and GSE203008). All four iPSC lines in every differentiation gave rise to secretory, basal, and multiciliated cells, and in five of eight differentiations, these four lines also gave rise to a transcriptionally discrete cluster of $FOXI1^+/CFTR^{hi}$ cells that coexpressed a diversity of ionocyte marker transcripts (Figures 1B–1E and E1D in the online supplemental). We visualized the transcriptomic programs of all cells derived in these five differentiations (Uniform Manifold Approximation and Projection; Figure 1B), and we identified six cell clusters (0–5) through Louvain clustering. We annotated each cluster on the basis of canonical airway lineage markers as defined in published lung cell atlases (1, 7, 8) (Figures 1B–1D). We observed a distinct cluster 5, composed of 182 cells (average frequency, 0.95% of all cells in each differentiation;

This article is open access and distributed under the terms of the Creative Commons Attribution Non-Commercial No Derivatives License 4.0. For commercial usage and reprints, please e-mail Diane Gern (dgern@thoracic.org).

Supported by the following grant awards: NIH HL155892 (R.W.); Alfred and Gilda Slifka Fund and CF/MS fund (T.S., Y.T., and R.W.); R01HL095993 (D.N.K.), CFF KOTTON20G0 (R.W., D.N.K., and F.J.H.), and R01HL139799 (F.J.H.). iPSC distribution and disease modeling is supported by NIH grants U01TR001810 and NO1 75N92020C00005 (D.N.K.). The authors thank Brian R. Tilton of the BUSM Flow Cytometry Core and Yuriy Alekseyev of the Boston University School of Medicine (BUSM) Sequencing Core.

Supplemental Figures can be found on our website: https://www.bumc.bu.edu/kottonlab/supplemental-figures-for-wang-kotton-el-2022

Originally Published in Press as DOI: 10.1164/rccm.202205-1010LE on March 1, 2023

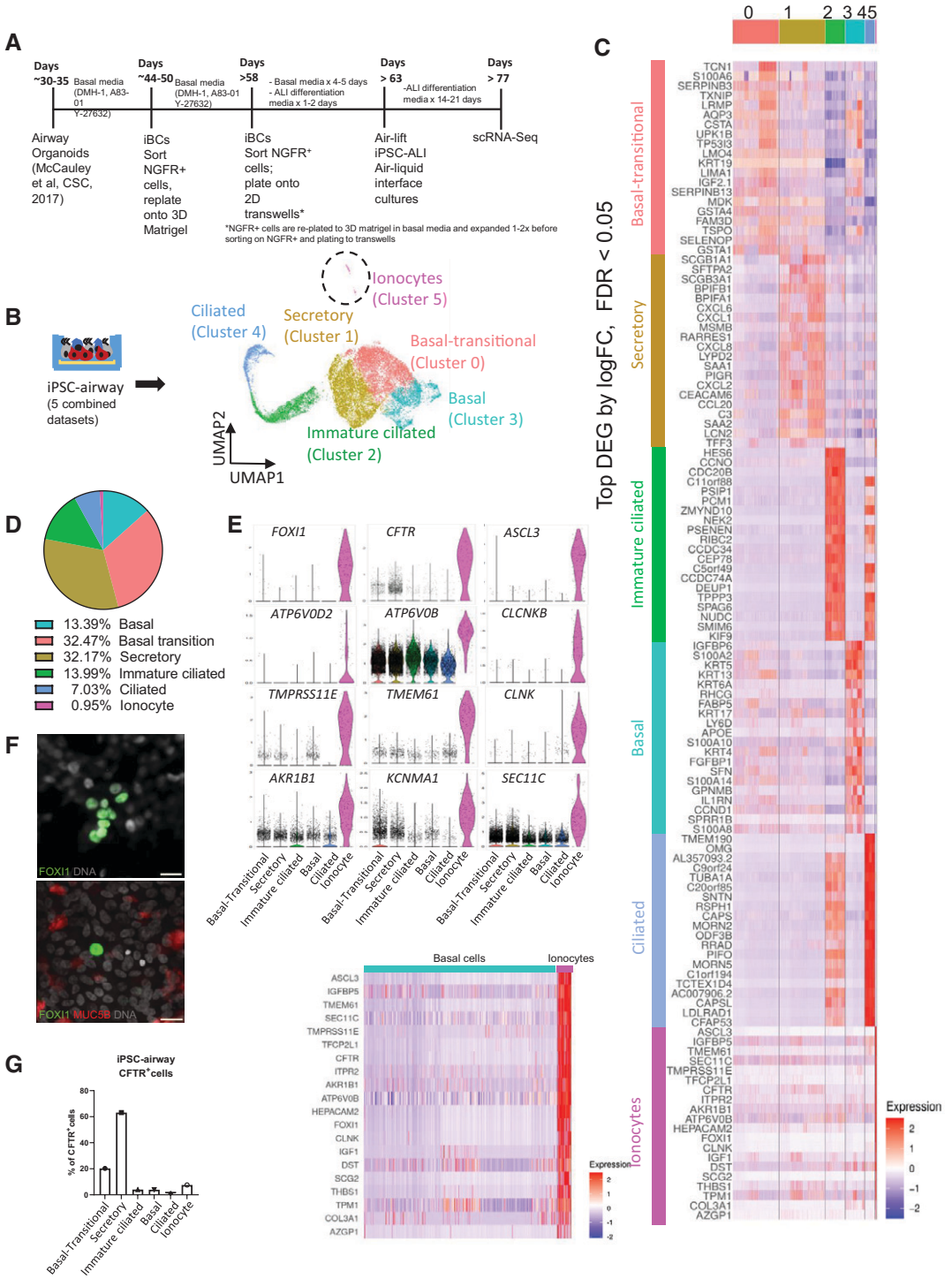


**Figure 1.** Directed differentiation of normal and cystic fibrosis induced pluripotent stem cells (iPSCs) into putative ionocytes. (*A*) Schematic of the six-stage iPSC-derived airway differentiation protocol. (*B*) UMAP with Louvain clustering (clusters 0–5) of five combined datasets of iPSC-derived differentiations after air–liquid interface (ALI) culture (cell lines 1,567 [F508del homozygous cystic fibrosis (CF)], 1,566 [1,567 CFTR (cystic fibrosis transmembrane conductance regulator)-corrected], 1,565 [F508del homozygous CF] repeated twice, 1,564 [1,565 CFTR-corrected]) cultured at ALI. (*C*) Right: Heatmap of top 20 differentially expressed genes (DEGs) in each cluster (FDR, <0.05; ranked by logFC per cluster). Left: Mini-heatmap of the expression of the top 20 ionocyte DEGs in the iPSC ionocyte and iPSC basal cells. (*D*) Cell lineage frequencies across all five combined datasets from *B*. (*E*) Violin plots comparing expression of ionocyte markers across cell clusters from *B*. (*F*) FOXI1 (forkhead box I1) nuclear protein immunostaining (green) (top/bottom) and MUC5B (red) (bottom) of iPSC-derived airway after ALI culture (iPSC line 1,566; gray, DNA; scale bar, 20 μm). (*G*) Distribution of CFTR$^{+}$ cells by airway cell type (cluster). FDR = false discovery rate; logFC = log fold change; UMAP = Uniform Manifold Approximation and Projection.

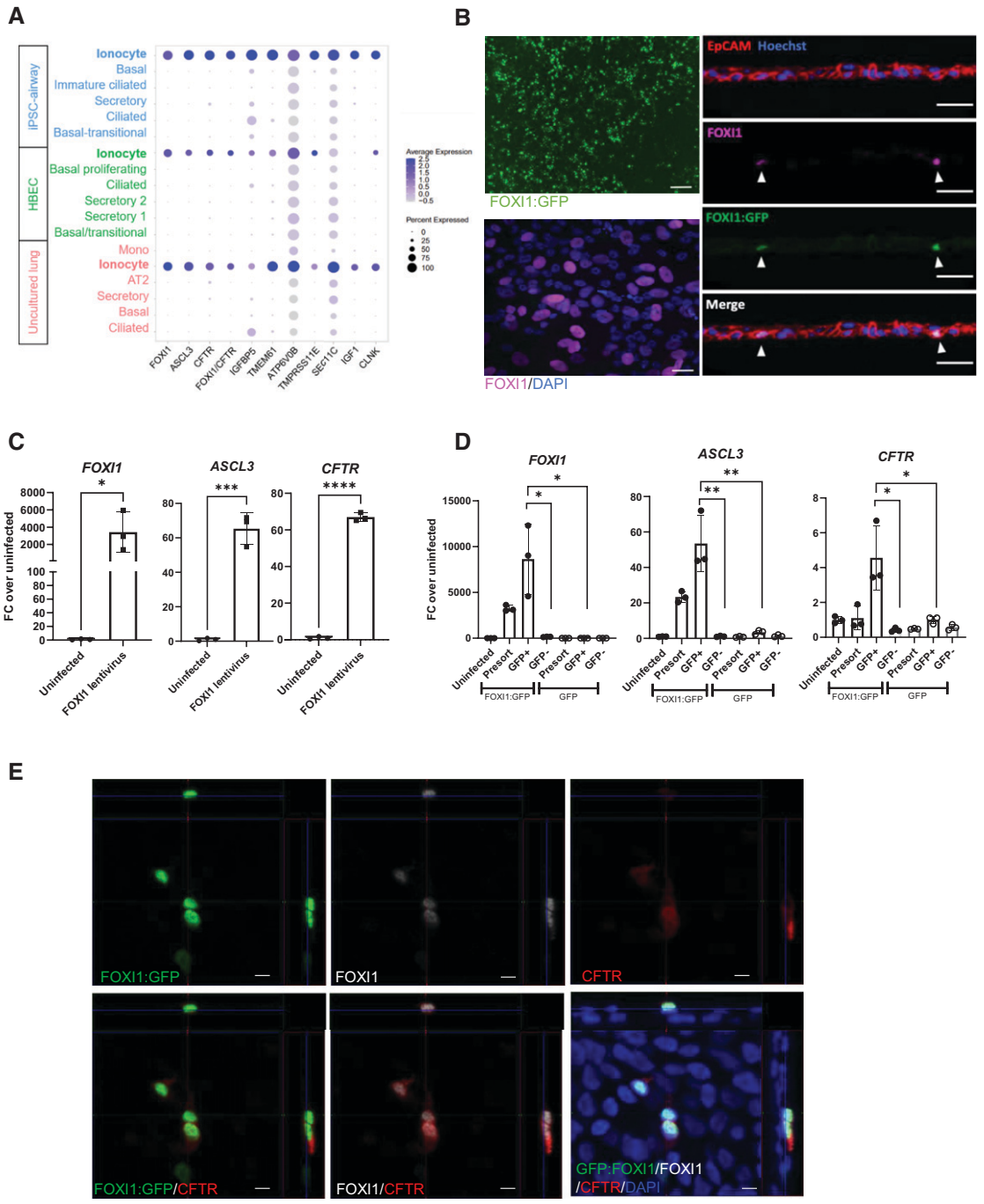


**Figure 2.** Comparison of primary and induced pluripotent stem cells (iPSC)-derived ionocytes and impact of FOXI1 (forkhead box I1) forced overexpression. (*A*) Dot plot comparing expression of each indicated ionocyte marker transcript across iPSC-derived airway cell types versus published uncultured (9) and cultured primary human bronchial epithelial cell (HBEC) (7) single-cell RNA sequencing datasets. HBECs after air–liquid interface (ALI) culture. (*B*) Immunofluorescence microscopy of two-dimensional cultures of iPSC-derived airway cells after transduction with lentiviral FOXI1:GFP (CFTR [cystic fibrosis transmembrane conductance regulator]-corrected line 1,566). Left: Low (left upper) and high (left lower; confocal microscopy) magnifications are shown of nuclear FOXI1$^{+}$ cells (purple). CFTR-corrected line 1,566; scale bars, 200 μm (left upper) and 10 μm (left lower). Blue = DAPI-stained cell nuclei. Right: Transverse sections of cryo-embedded iPSC airway (KOLF2-C1 line [13]; scale bars, 25 μm). (*C* and *D*) Gene expression quantitation by RT-qPCR of each indicated transcript in iPSC-derived airway cells transduced with either FOXI1:GFP or control GFP lentiviruses versus uninfected controls. FC expression compared with uninfected [$2^{-\Delta\Delta Ct}$] after 18S normalization is shown. $n = 3$ differentiations of CFTR-corrected line 1,566. (*E*) Immunofluorescence confocal microscopy of two-dimensional cultures (in ALI for 20 d) of iPSC airway cells after transduction with lentiviral FOXI1:GFP, showing immunostaining for GFP (upper left), FOXI1 (upper middle), and CFTR (upper right). Lower panels indicate colabeling of GFP/CFTR (lower left), FOXI1/CFTR (lower middle), and merged GFP/FOXI1/CFTR (lower right). Blue = DAPI-stained cell nuclei (CF line 007CF, generous gift of Amy Ryan; scale bars, 5 μm). FC = fold change. *$P \leq 0.05$; **$P \leq 0.01$; ***$P \leq 0.001$; ****$P \leq 0.0001$.

range, 0.34–1.67%), enriched in ionocyte markers, including *FOXI1*, *ASCL3*, *SEC11C*, *TMPRSS11E*, *TMEM61*, and *AKR1B1*, subunits of the vacuolar ATPase such as *ATP6V0B* and *ATP6V0D2* (Figures 1C, 1E, and E1A), alternative chloride channel *CLCNKB*, calcium-activated potassium channel *KCNMA1*, and *CFTR* (Figure 1E). The ~1% frequency of iPSC-derived putative ionocytes is consistent with published frequencies of primary ionocytes in mouse and human large airways (1, 2) and did not differ between CFTR mutant and corrected samples (Figure E1D). To validate FOXI1 expression on a protein level, we performed immunostaining, identifying rare cells expressing nuclear FOXI1 protein (Figure 1F).

As expected, we found more frequent representation of secretory, ciliated, and basal cell lineages in our profiles (Figure 1D), and we, therefore, assessed the expression of *CFTR* across these lineages relative to the rarer ionocytes. We found that 10% of all cells in our iBC-derived ALI cultures expressed detectable CFTR transcripts. *CFTR* expression levels were highest in iPSC-derived ionocytes per cell compared with other cell types, which is consistent with prior observations in primary cells (Figures 1E, E1A, and E1B) (1, 2). However, despite the high *CFTR* expression level in iPSC ionocytes, *CFTR* was expressed more frequently in other airway lineages, albeit at lower levels, with secretory cells composing the vast majority of all $CFTR^+$ iPSC-derived airway epithelia (Figures 1E, 1G, and E1A). We found no consistent statistically significant differences in CFTR expression (levels or frequencies) between cystic fibrosis and CFTR-corrected iPSC airways (Figure E1C). Specifically, counting all $CFTR^+$ cells, only 7.5% were ionocytes, whereas 63% were secretory cells, 20% were basal secretory transition cells, 3.9% were basal cells, 4% were immature ciliated cells, and 1% were mature ciliated cells (Figures 1E and 1G). Our data validate previous findings in primary airways that ionocytes express high levels of *CFTR* and make up only a small portion of $CFTR^+$ cells (1, 2, 6).

To compare iPSC-derived ionocytes with primary ionocytes, we quantified the expression levels and frequencies of ionocyte marker transcripts both in our cells and in annotated, published benchmark scRNA-Seq profiles of fresh (uncultured) human lung airway epithelia (9) and primary human bronchial epithelial cells after ALI culture (7). We found similar frequencies and expression levels of most ionocyte markers in iPSC-derived versus primary ionocytes, including *FOXI1*, *ASCL3*, *IGFBP5*, *TMEM61*, *TMPRSS11E*, *SEC11C*, *CLNK*, and *ATP6V0B* (Figure 2A). IGF1 (insulin-like growth factor 1) expression was lower and less frequent in cultured human bronchial epithelial cell–derived ionocytes, but it was similar between fresh and iPSC-derived ionocytes. Within the top 50 differentially expressed genes (DEGs) enriched in iPSC-derived ionocytes compared with all other iPSC-derived cell clusters, 70% (35 of 50) of genes were also found within the top 50 DEGs of at least one of these two primary datasets (data not shown). Furthermore, an unbiased comparison of iPSC-derived ionocyte transcriptomes (top 50 DEGs) with all available datasets from all tissues and lineages (Enrichr CellMarker Augmented 2021 database) indicated the most closely related transcriptome to be primary lung ionocytes (false discovery rate, $1 \times 10^{-89}$; Figure E1E).

Because ionocyte differentiation has been demonstrated to require Notch signaling (1), we investigated whether activating this pathway might be used to augment ionocyte differentiation and presence. We used an iPSC line with doxycycline-inducible NICD1 (NOTCH intracellular domain 1) targeted to the safe harbor AAVS1 human locus (Dox-NICD) (10) and differentiated the Dox-NICD iPSCs into airway epithelium (Figures E2A and E2B). Activation of NOTCH signaling in iBCs either before or during ALI differentiation led to increased basal cell differentiation into secretory cells at the expense of ciliated differentiation (Figures E2A and E2B), validating previous studies (11, 12). However, it did not lead to increased ionocytes or augmented FOXI1 expression (Figures E2A and E2B). Therefore, we concluded that in our system, NOTCH signaling is likely not sufficient for human ionocyte differentiation.

Finally, we tested the effect of forced overexpression of FOXI on ionocyte frequency in iPSC-derived cells, given that this approach generates more ionocytes in primary cell cultures, as demonstrated by Plasschaert and colleagues (1). We transduced iBCs in Transwells with a lentiviral vector encoding a FOXI1:GFP fusion cassette versus GFP-only control (OriGene, catalog no. RC218102L2V; multiplicity of infection, 1) (Figure 2B). *FOXI1* overexpression led to significantly increased expression of *ASCL3*, *FOXI1*, and *CFTR* (Figures 2C and 2D), and expression was enriched in $GFP^+$ cells sorted for analysis after FOXI1:GFP lentiviral transduction compared with $GFP^-$ cells or compared with $GFP^+$ cells transduced with the control GFP lentivirus (Figure 2D). At the protein level, we found colocalization of GFP, FOXI1, and CFTR by immunostaining (confocal immunofluorescence microscopy; Figure 2E).

Overall, our results indicate the successful directed differentiation of normal and cystic fibrosis iPSCs via iBCs into a human ionocyte-like population, providing a source of cells with relevance for basic studies and potential future applications for regenerative medicine. ■

**Author disclosures** are available with the text of this letter at www.atsjournals.org.

Correspondence and requests for reprints should be addressed to Ruobing Wang, M.D., Department of Pulmonary Medicine, Enders 414, 300 Longwood Ave, Boston, MA 02115 and Email: Ruobing.wang@childrens.harvard.edu. Darrell N. Kotton, M.D., Department of Pulmonary Medicine, Enders 414, 300 Longwood Ave, Boston, MA 02115. Email: dkotton@bu.edu.

## References

1. Plasschaert LW, Žilionis R, Choo-Wing R, Savova V, Knehr J, Roma G, *et al.* A single-cell atlas of the airway epithelium reveals the CFTR-rich pulmonary ionocyte. *Nature* 2018;560:377–381.
2. Montoro DT, Haber AL, Biton M, Vinarsky V, Lin B, Birket SE, *et al.* A revised airway epithelial hierarchy includes CFTR-expressing ionocytes. *Nature* 2018;560:319–324.
3. Travaglini KJ, Nabhan AN, Penland L, Sinha R, Gillich A, Sit RV, *et al.* A molecular cell atlas of the human lung from single-cell RNA sequencing. *Nature* 2020;587:619–625.
4. Quigley IK, Stubbs JL, Kintner C. Specification of ion transport cells in the *Xenopus* larval skin. *Development* 2011;138:705–714.
5. Vidarsson H, Westergren R, Heglind M, Blomqvist SR, Breton S, Enerbäck S. The forkhead transcription factor Foxi1 is a master regulator of vacuolar H-ATPase proton pump subunits in the inner ear, kidney and epididymis. *PLoS One* 2009;4:e4471.
6. Okuda K, Dang H, Kobayashi Y, Carraro G, Nakano S, Chen G, *et al.* Secretory cells dominate airway CFTR expression and function in human airway superficial epithelia. *Am J Respir Crit Care Med* 2021; 203:1275–1289.
7. Hawkins FJ, Suzuki S, Beermann ML, Barillà C, Wang R, Villacorta-Martin C, *et al.* Derivation of airway basal stem cells from human pluripotent stem cells. *Cell Stem Cell* 2021;28:79–95.e8.
8. Habermann AC, Gutierrez AJ, Bui LT, Yahn SL, Winters NI, Calvi CL, *et al.* Single-cell RNA sequencing reveals profibrotic roles of distinct

epithelial and mesenchymal lineages in pulmonary fibrosis. *Sci Adv* 2020;6:eaba1972.
9. Carraro G, Mulay A, Yao C, Mizuno T, Konda B, Petrov M, *et al.* Single-cell reconstruction of human basal cell diversity in normal and idiopathic pulmonary fibrosis lungs. *Am J Respir Crit Care Med* 2020;202:1540–1550.
10. Heinze D, Park S, McCracken A, Haratianfar M, Lindstrom J, Villacorta-Martin C, *et al.* Notch activation during early mesoderm induction modulates emergence of the T/NK cell lineage from human iPSCs. *Stem Cell Reports* 2022;17:2610–2628.
11. Tsao PN, Vasconcelos M, Izvolsky KI, Qian J, Lu J, Cardoso WV. Notch signaling controls the balance of ciliated and secretory cell fates in developing airways. *Development* 2009;136:2297–2307.
12. Rock JR, Gao X, Xue Y, Randell SH, Kong YY, Hogan BL. Notch-dependent differentiation of adult airway basal stem cells. *Cell Stem Cell* 2011;8:639–648.
13. Pantazis CB, Yang A, Lara E, McDonough JA, Blauwendraat C, Peng L, *et al.* A reference human induced pluripotent stem cell line for large-scale collaborative studies. *Cell Stem Cell* 2022;29:1685–1702.e22.

Copyright © 2023 by the American Thoracic Society

Check for updates

## Parasitic Infections and Biological Therapies Targeting Type 2 Inflammation: A VigiBase Study

Philippine Lifar[1]*, François Montastruc[2,3]*, Laurent L. Reber[4], Jean-François Magnaval[5], and Laurent Guilleminault[1,4]

[1]Department of Respiratory Medicine, [2]Department of Medical and Clinical Pharmacology, Centre of Pharmacovigilance and Pharmacoepidemiology, [5]Department of Clinical Parasitology, Faculty of Medicine, and [3]Centre of Clinical Investigation 1436, Team PEPSS "Pharmacology in Population cohortS and biobankS", Toulouse University Hospital Centre, Toulouse, France; and [4]Toulouse Institute for Infectious and Inflammatory Diseases (Infinity), Inserm U1291, University of Toulouse, CNRS U5282, F-CRIN CRISALIS, Toulouse, France

ORCID ID: 0000-0002-7344-8290 (L.G.).

*To the Editor*:

Severe asthma management has entered a new era with the approval of biological therapies (1, 2). The current approved biological therapies for severe asthma are omalizumab, an anti-IgE antibody; mepolizumab and reslizumab, anti–IL-5 antibodies; benralizumab, an anti–IL-5 receptor antibody; and dupilumab, an anti–IL-4 receptor antibody. These therapies are directed against type 2 inflammation driven by T-helper cell type 2 cells and innate lymphoid type 2 cells, both leading to the secretion of IL-5, IL-4, and IL-13 (2). Biological therapies have a significant impact on eosinophils and IgE that play a key role in severe asthma pathophysiology (3). However, it is well established that eosinophils are involved in the host response against parasitic infections, particularly helminths (4). Moreover, studies in mice indicate that IgE might be involved in the host's resistance to certain parasites by interacting with immune cells (5).

Given the role of type 2 inflammation in the defense against parasites (6), an increased risk of parasitic infections (particularly helminths) due to the use of biological therapies targeting type 2 inflammation has raised a safety concern. To address this question, we performed disproportionality analyses using VigiBase, the World Health Organization Global Database of Individual Case Safety Reports, to assess whether biological therapies (omalizumab, mepolizumab, benralizumab, and dupilumab) would be associated with a significant increase in reporting parasitic infections. The study protocol was approved by the institutional review board of the Société de Pneumologie de Langue Française (CEPRO 2019-041).

All reports of adverse events registered in VigiBase between January 1, 2006, and May 18, 2022, were considered. We included all reports pertaining to patients aged 18 years or older treated by at least one biological therapy approved for severe asthma. A control group, defined as reports associated with current approved inhaled therapies and the keyword "asthma" in the database, was used for the analysis. The outcomes of interest were parasitic infections according to the 10th revision of the International Classification of Diseases. Cases were identified by the presence of any parasitic infections according to the MedDRA dictionary (Medical Dictionary for Regulatory Activities).

Using a case/noncase design, we compared omalizumab or mepolizumab or benralizumab or dupilumab with the control group in terms of parasitic infections. We also compared the biological therapies with each other regarding any parasitic infections and specifically helminthiasis. Multivariable logistic regression was used to estimate adjusted odds ratios (aORs) with a 95% confidence interval (CI). aORs were adjusted on the following covariates: age, sex, and parasite-endemic countries.

We identified 90,704 patients with adverse events associated with omalizumab ($n = 18{,}352$), mepolizumab ($n = 6{,}731$), benralizumab ($n = 3{,}923$), dupilumab ($n = 42{,}482$), or the control group ($n = 19{,}349$) in VigiBase (Table 1). The proportion of reports coming from parasite-endemic countries ranged from 1.1% to 18.8%.

Among all reports of adverse events, the proportion of parasitic infections or helminthiasis was very low. In fact, a parasitic infection was noted in 4 (0.021%) controls, 11 (0.06%) patients treated with omalizumab, 5 (0.07%) treated with mepolizumab, 9 (0.23%) treated with benralizumab, and 15 (0.035%) treated with dupilumab. No difference regarding the rate of parasitic infection was seen between the control group and omalizumab or mepolizumab or dupilumab (aORs, 2.35 [95% CI, 0.78–8.61], 3.68 [95% CI, 0.97–5.32], and 1.50 [95% CI, 0.53–5.32], respectively) (Figure 1). However, parasitic infections were significantly more often reported with benralizumab than with the control group (aOR, 9.49 [95% CI, 3.08–35.07]). In relation to the comparison between the biological therapies, no difference was seen between dupilumab and omalizumab (aOR, 0.69 [95% CI, 0.31–1.62]) or mepolizumab and omalizumab (aOR, 1.71 [95% CI, 0.52–4.97]) or mepolizumab and dupilumab (aOR, 2.30 [95% CI, 0.73–6.15]). However, parasitic infections were significantly more often reported with benralizumab than with omalizumab or dupilumab (aORs, 3.99 [95% CI, 1.55–10.19] and 5.79 [95% CI, 2.39–13.31], respectively). The difference between benralizumab and mepolizumab was not significant (aOR, 02.89 [95% CI, 0.996–9.41]). All the results were similar regarding helminthiasis, but a significant increase in reporting helminthiasis infections with benralizumab was seen compared with mepolizumab (aOR, 11.39 [95% CI, 2.02–213.00]) (Figure 1).

Although the risk of parasitic infections has always been considered a theoretical adverse event of biological therapies

*Co–first authors.

Originally Published in Press as DOI: 10.1164/rccm.202210-1898LE on March 8, 2023